Progress of Theoretical Physics, Vol. 111, No. 1, January 2004

Chiral Sigma Model with Pion Mean Field in Finite Nuclei

Yoko Ogawa,[1,*)] Hiroshi Toki,[1,2,**)] Setsuo Tamenaga,[1] Hong Shen,[3] Atsushi Hosaka,[1] Satoru Sugimoto[2] and Kiyomi Ikeda[2]

[1] *Research Center for Nuclear Physics (RCNP), Osaka University, Ibaraki 567-0047, Japan*
[2] *Institute of Chemical and Physical Research (RIKEN), Wako 351-0198, Japan*
[3] *Department of Physics, Nankai University, Tianjin 300071, China*

(Received June 30, 2003)

The properties of infinite matter and finite nuclei are studied using the chiral sigma model in the framework of relativistic mean field theory. We reconstruct an extended chiral sigma model in which the omega meson mass is generated dynamically by sigma condensation in the vacuum in the same manner as the nucleon mass. All the parameters of the chiral sigma model are essentially fixed by the hadron properties in free space. In nuclear matter, the saturation property is described correctly, but the incompressibility is too large, and the scalar and vector potentials are about half as large as their phenomenological values. This fact is reflected in the properties of finite nuclei. We carry out calculations for $N = Z$ even-even mass nuclei between $N = 16$ and $N = 34$. The extended chiral sigma model without the pion mean field leads to the result that the magic number appears at $N = 18$, instead of $N = 20$, and the magic number does not appear at $N = 28$, due to the above mentioned nuclear matter properties. The latter problem, however, could be removed through the introduction of a finite pion mean field with the appearance of the magic number at $N = 28$. We find that the energy differences between the spin-orbit partners are reproduced by the finite pion mean field, which is a completely different mechanism from the standard spin-orbit interaction.

§1. Introduction

Chiral symmetry is known to be the most important symmetry in hadron physics. This is because quantum chromo-dynamics (QCD), in which the up and down quarks have essentially zero masses, is the underlying theory of the strong interaction. Chiral symmetry governs the quark dynamics. In the real world, quarks are confined and chiral symmetry is spontaneously broken. As the Nambu-Goldstone boson of the spontaneous breaking of chiral symmetry, the pion emerges with almost zero mass.

At the hadron level, chiral symmetry is described nicely by the linear sigma model introduced by Gell-Mann and Levy.[1)] Its non-linear version was proposed by Weinberg.[2)] Chiral symmetry and the generation of the hadron mass are described clearly in the Nambu-Jona-Lasinio Lagrangian with fermion fields.[3)] These Lagrangians have been used to describe various phenomena in hadron physics. We obtain a good description of the pion-nucleon properties in terms of these La-

*) E-mail: ogaway@rcnp.osaka-u.ac.jp
**) E-mail: toki@rcnp.osaka-u.ac.jp

grangians.[4] The pion, which was introduced by Yukawa as the mediator of the nucleon-nucleon interaction, received its foundation through spontaneous chiral symmetry breaking.[5]

It is then very natural to use the chiral sigma model Lagrangian for the description of nuclei. Such descriptions were derived by several groups employing the relativistic mean field approximation.[6)–10)] It was found that the chiral sigma model in its original form is not satisfactory for the description of nuclear matter. An interesting solution of this problem was proposed by Boguta et al., who introduced the dynamical generation of the omega meson mass in the same way as the nucleon mass.[7] They were able to reproduce the saturation properties of infinite matter with the extended chiral sigma (ECS) model. However, the effective mass predicted by their theory is too large and the incompressibility is very large. The extended chiral sigma model was applied to finite nuclei by Savushkin et al.[9),10)] The predicted binding energies are reasonable, but the spin-orbit splitting is too small in the RMF framework.

Recently, an interesting proposal was made regarding the role of the pion in finite nuclei by some of the present authors.[11] They carried out relativistic mean field calculations with a finite pion mean field using the TM1 parameter set.[12] In order to treat the pion mean field, they developed a formalism in which parity-mixed single particle states are introduced. Using the free space pion-nucleon coupling constant, they found that the pion mean field becomes finite. This effect appears to be particularly favorably for jj-closed shell nuclei, and the mass dependence of the energy gain associated with the pion behaves like the nuclear surface, $\langle V_\pi \rangle \sim A^{2/3}$. Hence, the name "surface pion condensation" was introduced for this phenomenon.

In this paper, we study the properties of infinite matter in terms of the ECS model by analyzing the non-linear equation of motion for the sigma field and obtain the saturation property of nuclear matter. We apply the ECS model to finite nuclei and study the properties of the binding energies and the single particle properties. Because the role of the finite pion mean field in determining the binding energies and the spin-orbit splitting is demonstrated in a recent publication,[11] we use the same formalism with the ECS model to treat the finite pion mean field. We study the appearance of the spin-orbit splitting due to the pion mean field by studying carefully the single particle spectra of finite nuclei.

In §2, we discuss the RMF formalism with the pion mean field. In §3, we study the saturation property of infinite nuclear matter with the original chiral sigma model and with the extended chiral sigma model. In §4, we study finite nuclei with the extended chiral sigma model without yes introducing the pion mean field and, further, study the properties of single particle states. Then, in §5, we introduce the finite pion mean field and discuss the mechanism of the appearance of the magic number effect and the energy splittings between the spin-orbit partners. We summarize the present study in §6, together with discussion of further study.

§2. Chiral sigma model in the relativistic mean field theory

We start with the linear sigma model with an omega meson field, which is defined by the following Lagrangian: [1)]

$$\begin{aligned}\mathcal{L}_{\sigma\omega} &= \bar{\Psi}(i\gamma_\mu\partial^\mu - g_\sigma(\sigma + i\gamma_5\vec{\tau}\cdot\vec{\pi}) - g_\omega\gamma_\mu\omega^\mu)\Psi \\ &+ \frac{1}{2}\partial_\mu\sigma\partial^\mu\sigma + \frac{1}{2}\partial_\mu\vec{\pi}\partial^\mu\vec{\pi} - \frac{\mu^2}{2}(\sigma^2+\vec{\pi}^2) - \frac{\lambda}{4}(\sigma^2+\vec{\pi}^2)^2 \\ &- \frac{1}{4}\omega_{\mu\nu}\omega^{\mu\nu} + \frac{1}{2}\widetilde{g_\omega}^2(\sigma^2+\vec{\pi}^2)\omega_\mu\omega^\mu \\ &+ \varepsilon\sigma. \end{aligned} \tag{2·1}$$

The fields Ψ, σ and π are the nucleon, sigma and pion fields. μ and λ are the sigma model coupling constants. Here we have introduced the explicit chiral symmetry breaking term $\varepsilon\sigma$ and, in addition, the mass generation term for the omega meson due to the sigma meson condensation, as in the case of the nucleon mass in free space. [7)] The σ-ω coupling term of this structure can be derived from the bosonization [13)] of the Nambu-Jona-Lasinio model. [3)]

In a finite nuclear system, it is believed to be necessary to use the non-linear representation of the chiral symmetry. This is because the pseudoscalar pion-nucleon coupling in the linear sigma model makes the coupling of the positive and negative energy states extremely strong, and we have to treat the negative energy states very carefully. We can derive the non-linear sigma model by introducing new variables and making a suitable transformation,

$$\begin{aligned} \sigma + i\vec{\tau}\cdot\vec{\pi} &= \rho U, \qquad & U &= e^{i\vec{\tau}\cdot\vec{\pi}/f_\pi}, \\ \sigma + i\gamma_5\vec{\tau}\cdot\vec{\pi} &= \rho U_5, \qquad & U_5 &= e^{i\gamma_5\vec{\tau}\cdot\vec{\pi}/f_\pi}. \end{aligned} \tag{2·2}$$

We further implement the Weinberg transformation for the nucleon field as $\psi = \sqrt{U_5}\Psi$. We then obtain the sigma-omega model Lagrangian in non-linear representation,

$$\begin{aligned}\mathcal{L}'_{\sigma\omega} &= \bar{\psi}(i\gamma_\mu\partial^\mu - g_\sigma\rho - \gamma_\mu v^\mu - \gamma_5\gamma_\mu a^\mu - g_\omega\gamma_\mu\omega^\mu)\psi \\ &+ \frac{1}{2}\partial_\mu\rho\partial^\mu\rho + \frac{\rho^2}{4}\mathrm{tr}\partial_\mu U\partial^\mu U^\dagger - \frac{\mu^2}{2}\rho^2 - \frac{\lambda}{4}\rho^4 \\ &- \frac{1}{4}\omega_{\mu\nu}\omega^{\mu\nu} + \frac{1}{2}\widetilde{g_\omega}^2\rho^2\omega_\mu\omega^\mu + \varepsilon\rho\frac{1}{2}(U+U^\dagger). \end{aligned} \tag{2·3}$$

In the above Lagrangian, the vector field v^μ and the axial vector field a^μ contain the pion terms. The vector and axial vector fields are expanded in terms of the pion field as

$$\begin{aligned} v^\mu &= \frac{-i}{8{f_\pi}^2}(\vec{\tau}\cdot\vec{\pi}\vec{\tau}\cdot\partial^\mu\vec{\pi} - \vec{\tau}\cdot\partial^\mu\vec{\pi}\vec{\tau}\cdot\vec{\pi}) + \cdots, \\ a^\mu &= \frac{1}{2f_\pi}\vec{\tau}\cdot\partial^\mu\vec{\pi} + \cdots. \end{aligned} \tag{2·4}$$

The kinetic term is expanded as

$$\frac{\rho^2}{4}\mathrm{tr}\partial_\mu U\partial^\mu U^\dagger = \frac{\rho^2}{2{f_\pi}^2}\partial_\mu\vec{\pi}\partial^\mu\vec{\pi} + \mathcal{O}(\vec{\pi}^4) + \mathcal{O}(\vec{\pi}^6) + \cdots, \tag{2·5}$$

and the explicitly chiral symmetry breaking term is expanded as

$$\varepsilon\rho\frac{1}{2}(U+U^\dagger) = \varepsilon\rho\left(1 - \frac{1}{2{f_\pi}^2}\vec{\pi}^2 + \frac{1}{24{f_\pi}^4}\vec{\pi}^4 + \cdots\right). \tag{2·6}$$

We now take the lowest-order terms in the pion field and omit higher-order terms. The resulting Lagrangian is written

$$\begin{aligned}\mathcal{L}'_{\sigma\omega} = {}& \bar{\psi}\left(i\gamma_\mu\partial^\mu - g_\sigma\rho - \frac{1}{2f_\pi}\gamma_5\gamma_\mu\vec{\tau}\cdot\partial^\mu\vec{\pi} - g_\omega\gamma_\mu\omega^\mu\right)\psi \\ &+ \frac{1}{2}\partial_\mu\rho\partial^\mu\rho + \frac{1}{2}\frac{\rho^2}{{f_\pi}^2}\partial_\mu\vec{\pi}\partial^\mu\vec{\pi} - \frac{\mu^2}{2}\rho^2 - \frac{\lambda}{4}\rho^4 \\ &- \frac{1}{4}\omega_{\mu\nu}\omega^{\mu\nu} + \frac{1}{2}\widetilde{g_\omega}^2\rho^2\omega_\mu\omega^\mu + \varepsilon\rho\left(1 - \frac{1}{2{f_\pi}^2}\vec{\pi}^2\right).\end{aligned} \tag{2·7}$$

We now take the vacuum expectation value of the ρ field to be f_π, which is determined by the pion decay rate:[4)]

$$\langle\rho\rangle_0 = f_\pi. \tag{2·8}$$

A new fluctuation field φ is then defined by the equation

$$\rho = f_\pi + \varphi. \tag{2·9}$$

We now rewrite the Lagrangian (2.7) in terms of the new field φ:

$$\begin{aligned}\mathcal{L}'_{\sigma\omega} = {}& \bar{\psi}\left(i\gamma_\mu\partial^\mu - g_\sigma f_\pi - g_\sigma\varphi - \frac{1}{2f_\pi}\gamma_5\gamma_\mu\vec{\tau}\cdot\partial^\mu\vec{\pi} - g_\omega\gamma_\mu\omega^\mu\right)\psi \\ &+ \frac{1}{2}\partial_\mu\varphi\partial^\mu\varphi + \frac{1}{2}\left(1+\frac{\varphi}{f_\pi}\right)^2\partial_\mu\vec{\pi}\partial^\mu\vec{\pi} - \frac{\mu^2}{2}(f_\pi+\varphi)^2 - \frac{\lambda}{4}(f_\pi+\varphi)^4 \\ &- \frac{1}{4}\omega_{\mu\nu}\omega^{\mu\nu} + \frac{1}{2}\widetilde{g_\omega}^2(f_\pi+\varphi)^2\omega_\mu\omega^\mu \\ &+ \varepsilon(f_\pi+\varphi)\left(1 - \frac{1}{2{f_\pi}^2}\vec{\pi}^2\right).\end{aligned} \tag{2·10}$$

Here, we have dropped a non-essential c-number constant. We find that the term φ/f_π is small and drop it by employing the approximations

$$\begin{aligned}\frac{1}{2}\left(1+\frac{\varphi}{f_\pi}\right)^2\partial_\mu\vec{\pi}\partial^\mu\vec{\pi} &\approx \frac{1}{2}\partial_\mu\vec{\pi}\partial^\mu\vec{\pi}, \\ \left(1+\frac{\varphi}{f_\pi}\right)\frac{1}{2}\frac{\varepsilon}{f_\pi}\vec{\pi}^2 &\approx \frac{1}{2}\frac{\varepsilon}{f_\pi}\vec{\pi}^2.\end{aligned} \tag{2·11}$$

We have to set the dangerous term, that is, the term linear in φ, equal to zero. This leads to the energy minimum condition,

$$\begin{aligned}(\varepsilon - {m_\pi}^2 f_\pi)\varphi &\longrightarrow 0,\\ {m_\pi}^2 &= \frac{\varepsilon}{f_\pi}.\end{aligned} \tag{2·12}$$

Finally, the Lagrangian for the new field φ with the above approximations is given as

$$\begin{aligned}\mathcal{L}'_{\sigma\omega} = \bar{\psi}\Big(& i\gamma_\mu\partial^\mu - M - g_\sigma\varphi - \frac{1}{2f_\pi}\gamma_5\gamma_\mu\vec{\tau}\cdot\partial^\mu\vec{\pi} - g_\omega\gamma_\mu\omega^\mu\Big)\psi\\ & + \frac{1}{2}\partial_\mu\varphi\partial^\mu\varphi - \frac{1}{2}{m_\sigma}^2\varphi^2 - \lambda f_\pi\varphi^3 - \frac{\lambda}{4}\varphi^4\\ & + \frac{1}{2}\partial_\mu\vec{\pi}\partial^\mu\vec{\pi} - \frac{1}{2}{m_\pi}^2\vec{\pi}^2\\ & - \frac{1}{4}\omega_{\mu\nu}\omega^{\mu\nu} + \frac{1}{2}{m_\omega}^2\omega_\mu\omega^\mu + {\widetilde{g_\omega}}^2 f_\pi\varphi\omega_\mu\omega^\mu + \frac{1}{2}{\widetilde{g_\omega}}^2\varphi^2\omega_\mu\omega^\mu,\end{aligned} \tag{2·13}$$

where we have set $M = g_\sigma f_\pi$, ${m_\pi}^2 = \mu^2 + \lambda {f_\pi}^2$, ${m_\sigma}^2 = \mu^2 + 3\lambda {f_\pi}^2$ and $m_\omega = \widetilde{g_\omega} f_\pi$. The effective masses of the nucleon and omega meson are given by $M^* = M + g_\sigma\varphi$ and ${m_\omega}^* = m_\omega + \widetilde{g_\omega}\varphi$, respectively. We take the masses and the pion decay constant as $M = 939$ MeV, $m_\omega = 783$ MeV, $m_\pi = 139$ MeV, and $f_\pi = 93$ MeV. Then, the other parameters can be fixed automatically using the relations $g_\sigma = M/f_\pi = 10.1$ and $\widetilde{g_\omega} = m_\omega/f_\pi = 8.42$. The strengths of the cubic and quadratic sigma meson self-interactions depend on the sigma meson mass through the relation $\lambda = ({m_\sigma}^2 - {m_\pi}^2)/2{f_\pi}^2$ in the chiral sigma model. The mass of the sigma meson, m_σ, and the coupling constant of the omega and nucleon, g_ω, are the free parameters. If we use the KSFR relation for the omega meson,[14),17)] and the additional relation from the Nambu-Jona-Lasinio model, the mass of the omega meson is related to the pion decay constant as $m_\omega = (2\sqrt{2}/3)f_\pi g_\omega$. Here, the factor $(2\sqrt{2}/3)$ stems from the relation $g_\omega = (3/2)g$, where g is the universal coupling constant for the vector meson.[15),16)] As we see below, this KSFR relation is satisfied in the present model to within 6%.

§3. Extended chiral sigma model for infinite matter

We first apply the extended chiral sigma model to infinite matter. It is important to reproduce the saturation properties of infinite nuclear matter first. Otherwise, we do not obtain convergence, due to the existence of multiple solutions in the Hartree calculation for finite systems. We assume that the pion mean field vanishes in infinite matter. Hereafter, we write the scalar meson field φ in the Lagrangian (2·13) as σ, because σ is used usually as the scalar meson field in relativistic mean field theory. The equations of motion for the nucleon field and the meson fields are written

$$\begin{aligned}(i\gamma_\mu\partial^\mu - M - g_\sigma\sigma - g_\omega\gamma^0\omega)\psi &= 0,\\ {m_\sigma}^2\sigma + 3\lambda f_\pi\sigma^2 + \lambda\sigma^3 - {\widetilde{g_\omega}}^2 f_\pi\omega^2 - {\widetilde{g_\omega}}^2\sigma\omega^2 &= -g_\sigma\rho_s,\\ {m_\omega}^2\omega + 2{\widetilde{g_\omega}}^2 f_\pi\sigma\omega + {\widetilde{g_\omega}}^2\sigma^2\omega &= g_\omega\rho_v,\end{aligned} \tag{3·1}$$

with

$$\rho_s = \frac{4}{(2\pi)^3}\int^{k_{\rm F}} d^3k \frac{M^*}{\sqrt{k^2+M^{*2}}}$$
$$= \frac{M^*}{\pi^2}\left\{k_{\rm F}\sqrt{{k_{\rm F}}^2+M^{*2}} - M^{*2}\log\left|\frac{k_{\rm F}+\sqrt{{k_{\rm F}}^2+M^{*2}}}{M^*}\right|\right\}, \tag{3·2}$$

$\rho_v = 2{k_{\rm F}}^3/(3\pi^2)$, and the effective mass of the nucleon $M^* = M + g_\sigma\sigma$. We note here that now the equations of motion of the sigma and omega mesons are coupled, due to the dynamical mass generation term of the omega meson. This sigma-omega coupling plays an important role in obtaining a reasonable equation of state for nuclear matter.

We first discuss the original chiral sigma model for the nuclear matter calculation.[7] In this case, there is no coupling between the equations for the sigma and omega fields. The equation for σ is a third-order algebraic equation in the sigma together with the opposite of the scalar coupling times the scalar density, $-g_\sigma\rho_s$, which is a function of the sigma field for a fixed density:

$$m_\sigma^2\sigma + 3\lambda f_\pi\sigma^2 + \lambda\sigma^3 = -g_\sigma\rho_s. \tag{3·3}$$

The right-hand side increases as the sigma field decreases and changes sign near $\sigma = -f_\pi \sim -0.5$ fm^{-1}. We focus on the solution above the crossing point, below which the effective mass of the nucleon is positive. Below a certain density, there appears only one solution, while above this density there appear three solutions. We obtain multiple solutions, as discussed above. For each solution, there is a

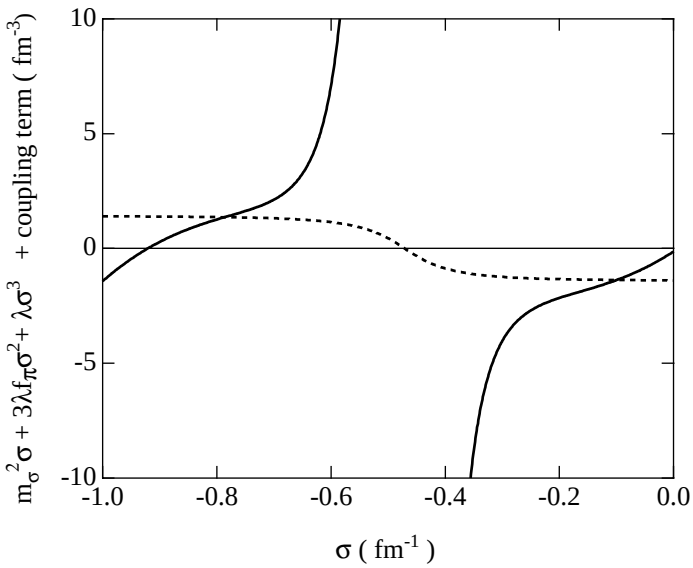

Fig. 1. The equation for σ with the σ-ω coupling term in the case $\rho = 0.141$ fm^{-3} for the extended chiral sigma model. There is one solution for each density continuously from zero density.

corresponding energy, which is not a smooth function of the density. Hence, we are not able to obtain good behavior for the equation of state with the original chiral sigma model.

A method for obtaining good nuclear matter properties was suggested by Boguta, who introduced the dynamical omega meson term.[7] The omega mass appears due to the dynamical chiral symmetry breaking, and hence there is a coupling between the sigma and the omega fields. We use this extended chiral sigma model for nuclear matter. The additional term provides a pole at the point where the effective nucleon mass is zero, $\sigma = -f_\pi$, as shown in Fig. 1. For this reason, we find a solution at a small value of sigma for each density continuously from zero. We are therefore able to obtain a reasonable energy per particle in the entire density region for infinite matter.

In Fig. 2 we display the energy per particle of nuclear matter as a function of the density for the extended chiral sigma model. We take the parameters of the chiral sigma model from the properties of mesons as the pion mass, m_π, the omega meson mass, m_ω, and the pion decay constant, f_π. The free parameters, m_σ and g_ω, are adjusted to realize the saturation property in the case of the extended chiral sigma model. We fix the free parameters as $m_\sigma = 777$ MeV and $g_\omega = 7.03$. Then, the strengths of the cubic and quadratic sigma meson self-interactions are fixed as $\lambda = 33.8$. The saturation properties are the density, $\rho = 0.141$ fm^{-3}, and the energy per particle, $E/A = -16.1$ MeV. We find the incompressibility in this case to be $K = 650$ MeV. The sigma meson mass chosen here is larger than that used in the one-boson exchange potential, which is around 500 MeV. If we use 500 MeV as the sigma

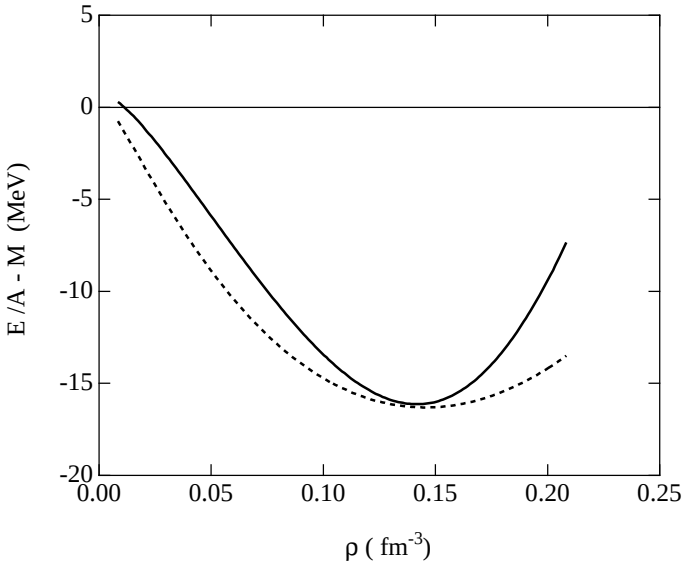

Fig. 2. The energy per particle of infinite nuclear matter as a function of the density for the extended chiral sigma model (solid curve). As a reference, the energy per particle obtained from the RMF theory with the TM1 parameter set, RMF(TM1), is displayed by the dashed curve.

meson mass, the attractive force becomes strong, and the saturation curve becomes deep. Therefore, we adjust the omega-nucleon coupling constant g_ω to reproduce the binding energy per particle. The energy minimum point appears at quite a small density, $\rho = 0.053$ fm^{-3}. The saturation condition is not satisfied simultaneously for the density and binding energy per particle using this meson mass. It is interesting that the value $m_\sigma = 777$ MeV is very close to that in the case that the chiral mixing angle is chosen at 45° in the generalized chiral model: $m_\sigma \approx m_\rho$.[2)]

As a comparison, the energy per particle of the mean field result with the TM1 parameter set is plotted together with the present result.[12)] The RMF(TM1) calculation reproduces the results of the relativistic Brueckner-Hartree-Fock calculation.[19)] We see that the present equation of state is much harder than taht of RMF(TM1). The incompressibility is found to be 650 MeV, while it is 281 MeV for TM1. In Fig. 3, we plot the vector and the scalar potentials and compare with those of RMF(TM1). The values found are about half as large as those in the case of the TM1 parameter set. This is because the extended chiral sigma model has solutions at smaller values of sigma than does RMF(TM1).

We note the consequence of the smaller absolute values of the scalar and vector potentials in finite nuclei as shown in Fig. 3. The summation of the absolute values of the scalar and vector potentials is directly related to the spin-orbit potential of finite nuclei. Hence, the fact that these absolute values are about half as large as the values for RMF(TM1) indicates that the spin-orbit splitting for finite nuclei should be about half as large as the necessary spin-orbit splittings.

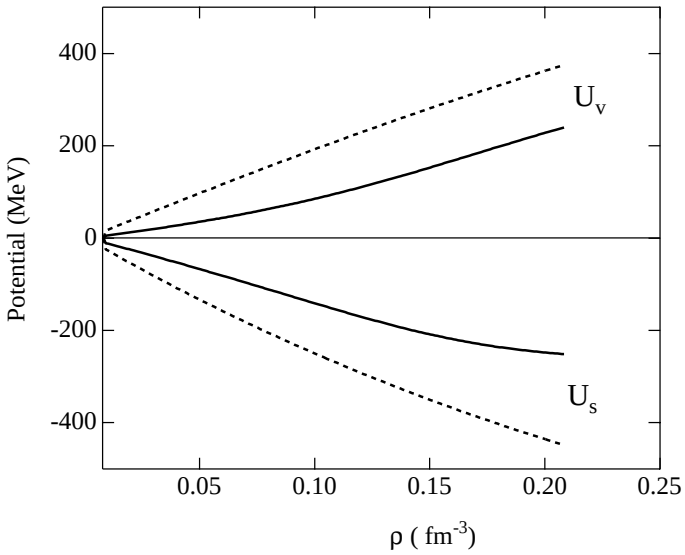

Fig. 3. The scalar and vector potentials as functions of the density for the extended chiral sigma model represented by the solid curves and those for RMF(TM1) represented by the dashed curves.

§4. Extended chiral sigma model for finite nuclei

We are now in a position to apply the extended chiral sigma (ECS) model, which is able to realize a saturation property with the above mentioned features in the case of finite nuclei. For this purpose, we consider $N = Z$ even-even mass nuclei to avoid the complication arising from the isovector part of the nucleon-nucleon interaction. We carry out calculations for these nuclei using the RMF framework with the ECS Lagrangian and compare the results with those of the standard RMF calculation employing the TM1 parameter set. Because the role of the pion mean field in determining the binding energy and the spin-orbit interaction is demonstrated in Ref. 11) for finite nuclei, we introduce the RMF formalism for the treatment of the finite pion mean field and study the effect of the finite pion mean field on the nuclear properties.

We here write the RMF equations for finite nuclei with a pion mean field. The Euler-Lagrange equation yields the Dirac equation for the nucleon,

$$\left(- i\vec{\alpha} \cdot \nabla + \gamma_0(M + g_\sigma \sigma) + g_\omega \omega + \frac{g_A}{2f_\pi}\gamma_0\gamma_5\vec{\gamma} \cdot \tau^0 \nabla\pi \right)\psi = \varepsilon\psi, \tag{4·1}$$

and the Klein-Gordon equations for the mesons,

$$(-\nabla^2 + {m_\pi}^2)\pi = \frac{g_A}{2f_\pi}\rho_{pv}, \tag{4·2}$$

$$(-\nabla^2 + {m_\sigma}^2)\sigma = -g_\sigma\rho_s - 3\lambda f_\pi \sigma^2 - \lambda\sigma^3 + \widetilde{g_\omega}^2 f_\pi \omega^2 + \widetilde{g_\omega}^2 \sigma\omega^2, \tag{4·3}$$

$$(-\nabla^2 + {m_\omega}^2)\omega = g_\omega\rho_v - 2\widetilde{g_\omega}^2 f_\pi \sigma\omega - \widetilde{g_\omega}^2 \sigma^2\omega, \tag{4·4}$$

where we consider an isospin symmetric nucleus, i.e. $N = Z$. There is a symmetry theorem for the Hartree-Fock (mean field) approximation with respect to the symmetry of the original Lagrangian.[20),21)] In the isospin symmetric nuclear case, we can verify that the mean field Lagrangian is symmetric under isospin rotation mixing the proton and neutron states. Hence, we can consider a special case, that in which only π^0 is finite, due to the isospin symmetry of the mean field Lagrangian, and write it as π. In fact, we have checked this symmetry by performing mean field calculations with π^0 in one case and with $\pi^\pm$ in another case and obtained the same energy in both cases.[11)] When we go beyond the mean field approximation, we have to include all the charge states of pion in the charge and parity projected mean field method, which is beyond the scope of this paper. We employ the static approximation and assume the time reversal symmetry of the system. Here we have introduced g_A in the pion nucleon coupling in order to satisfy the Goldberger-Treiman relation. In the linear sigma model, we obtain $g_A = 1$. In the mean field approximation, the source terms of the Klein-Gordon equations are replaced by their expectation values in the ground state:

$$\frac{g_A}{2f_\pi}\nabla \cdot \bar{\psi}\gamma_5\vec{\gamma}\tau^0\psi \longrightarrow \frac{g_A}{2f_\pi}\langle \nabla \cdot \bar{\psi}\gamma_5\vec{\gamma}\tau^0\psi\rangle = \frac{g_A}{2f_\pi}\rho_{pv}, \tag{4·5}$$

$$g_\sigma\bar{\psi}\psi \longrightarrow g_\sigma\langle\bar{\psi}\psi\rangle = g_\sigma\rho_s, \tag{4·6}$$

$$g_\omega\bar{\psi}\gamma_0\psi \longrightarrow g_\omega\langle\bar{\psi}\gamma_0\psi\rangle = g_\omega\rho_v. \tag{4·7}$$

The total energy is given by

$$
\begin{aligned}
E_{\text{total}} &= \int d^3r\mathcal{H} \\
&= \sum_{njm} \varepsilon_{njm} - \int d^3r \Big\{ \frac{1}{2} g_\sigma \rho_s \sigma + \frac{1}{2} g_\omega \rho_v \omega - \frac{1}{2} \frac{g_{\text{A}}}{2 f_\pi} \rho_{pv} \pi \\
&\qquad + \frac{1}{6}(3\lambda f_\pi)\sigma^3 + \frac{\lambda}{4}\sigma^4 - \frac{1}{2}\widetilde{g_\omega}^2 f_\pi \sigma \omega^2 - \frac{1}{2}\widetilde{g_\omega}^2 \sigma^2 \omega^2 \Big\} \\
&\qquad - ZM_p - ZM_n - E_{\text{c.m.}},
\end{aligned}
\tag{4·8}
$$

where we take the center-of-mass correction as $E_{\text{c.m.}} = \frac{3}{4}(41A^{\frac{1}{3}})$ MeV. Here we use the wave functions and densities for the case of a finite pion mean field. In this case, the parity of the nucleon is broken, because the pion source term has negative parity. The nucleon wave functions are then written

$$
\psi_{njmm_\tau} = \begin{pmatrix} iG_{n\kappa m_\tau}\mathcal{Y}_{\kappa m}\zeta(m_\tau) + iG_{n\bar{\kappa} m_\tau}\mathcal{Y}_{\bar{\kappa} m}\zeta(m_\tau) \\ F_{n\kappa m_\tau}\mathcal{Y}_{\bar{\kappa} m}\zeta(m_\tau) + F_{n\bar{\kappa} m_\tau}\mathcal{Y}_{\kappa m}\zeta(m_\tau) \end{pmatrix}, \tag{4·9}
$$

where the summation over κ represents the parity mixing, where κ is $\kappa = -(l_\uparrow + 1)$ for $l_\uparrow = j - 1/2$ and $\kappa = l_\downarrow$ for $l_\downarrow = j + 1/2$. Using these wave functions, we can calculate all the necessary densities as

$$
\rho_s = \sum_{nj} W_{nj} \frac{2j+1}{4\pi} \sum_{m_\tau} (|G_{n\kappa m_\tau}|^2 - |F_{n\kappa m_\tau}|^2 + |G_{n\bar{\kappa} m_\tau}|^2 - |F_{n\bar{\kappa} m_\tau}|^2), \tag{4·10}
$$

$$
\rho_v = \sum_{nj} W_{nj} \frac{2j+1}{4\pi} \sum_{m_\tau} (|G_{n\kappa m_\tau}|^2 + |F_{n\kappa m_\tau}|^2 + |G_{n\bar{\kappa} m_\tau}|^2 + |F_{n\bar{\kappa} m_\tau}|^2), \tag{4·11}
$$

$$
\begin{aligned}
\rho_{pv} &= -2 \sum_{nj} W_{nj} \frac{2j+1}{4\pi} \\
&\quad \times \sum_{m_\tau} (-1)^{\frac{1}{2} - m_\tau} \Big\{ \frac{d}{dr}(G_{n\kappa m_\tau}{}^* G_{n\bar{\kappa} m_\tau}) + \frac{2}{r}(G_{n\kappa m_\tau}{}^* G_{n\bar{\kappa} m_\tau}) \\
&\qquad + \frac{d}{dr}(F_{n\kappa m_\tau}{}^* F_{n\bar{\kappa} m_\tau}) + \frac{2}{r}(F_{n\kappa m_\tau}{}^* F_{n\bar{\kappa} m_\tau}) \Big\}.
\end{aligned}
\tag{4·12}
$$

We are now able to solve the coupled differential equations by carrying out iterative calculations.

In this section, we first discuss the properties of finite nuclei in terms of the extended chiral sigma model without yet introducing the pion mean field. We present the results for the binding energies per particle for $N = Z$ even-even mass nuclei from $N = 16$ up to $N = 34$ in Fig. 4. We take all the parameters of the extended chiral sigma model to be those of nuclear matter (Figs. 2 and 3), except that we use $g_\omega = 7.176$ instead of 7.033 to obtain overall agreement with the RMF(TM1) results. We include the Coulomb intereaction in the actual calculations. For comparison,

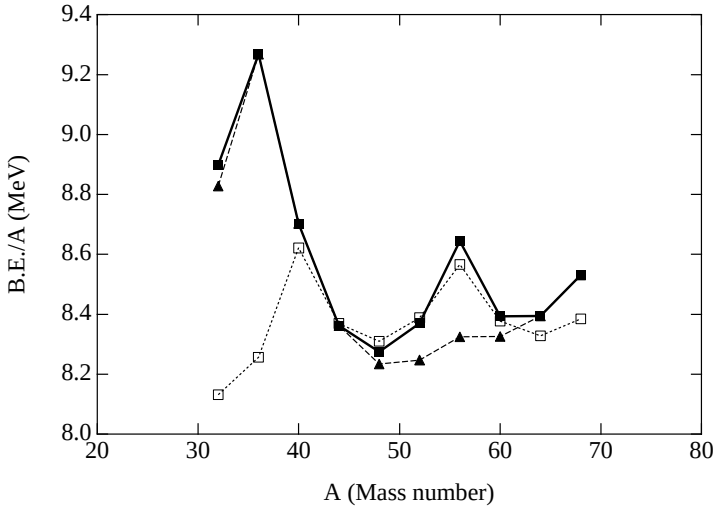

Fig. 4. The binding energy per particle for $N = Z$ even-even mass nuclei in the neutron number range of $N = 16 - 34$. The binding energies per particle for the case of the extended chiral sigma model without and with the pion mean field are represented by the dashed and the solid curves. As a comparison, those for the RMF(TM1) are represented by the dotted line.

we carry out calculations for these nuclei employing the RMF approximation with neither pairing nor deformation. The RMF(TM1) provides the magic numbers, which are indicated as the binding energy per particle increases at $N = Z = 20$ and 28. The extended chiral sigma model without the pion mean field, however, provides the magic number behavior only at $N = Z = 18$, instead of $N = Z = 20$.

In order to see how the difference between the two models for the Lagrangian arises, we show in Fig. 5 the single particle levels for the two models. In the case of the TM1 parameter set, displayed in Fig. 5, the shell gaps are clearly visible at $N = 20$ and 28. The magic number at $N = 20$ is due to the central potential, while the magic number at $N = 28$ comes from the spin-orbit splitting of the $0f$-orbit. This is definitely due to the fact that the vector potential and scalar potential in nuclear matter are large, so as to provide a large spin-orbit splitting. The situation for the single particle spectrum of the extended chiral sigma model is quite different from this case, as seen in Fig. 6. The most distinctive feature is that the $1s_{1/2}$ orbit is pushed up significantly. For this reason, the $0d_{3/2}$ orbit becomes the magic shell at $N = 18$, and a magic number appears at $N = 18$ instead of $N = 20$. We also see that there is no strong spin-orbit splitting, and hence there appears no shell gap at $N = 28$. The first discrepancy could be due to the large incompressibility, as seen in the nuclear matter energy per particle shown in Fig. 2. The other is due to the relatively small vector and scalar potentials in nuclear matter, as seen in Fig. 3.

We now give more detailed discussion of the spin-orbit splitting in the situation that the compressibility is very large, as in the ECS model, because the spin-orbit splitting is related to the behavior of the scalar-vector potential difference in the surface region. We show in Fig. 7 how the scalar-vector potential difference behaves

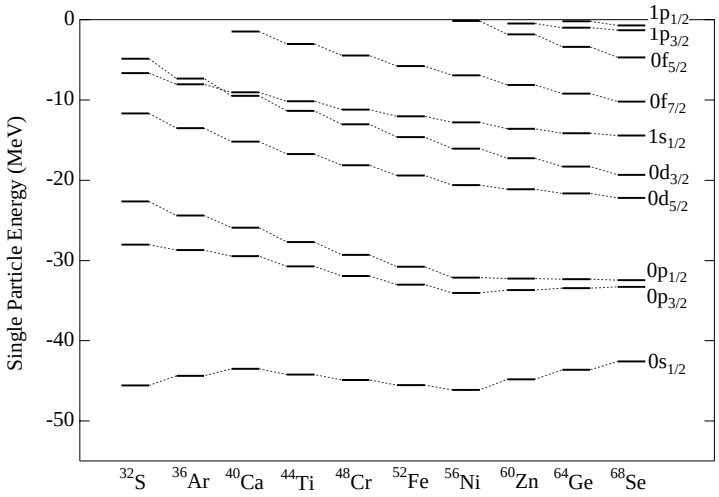

Fig. 5. The proton single particle energies for $N = Z$ even-even mass nuclei in the case of the RMF(TM1) theory. The magic numbers at $N = 20$ and 28 are visible.

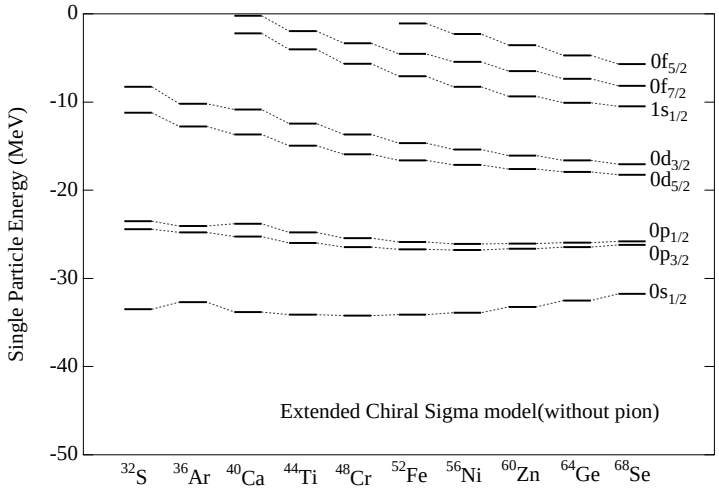

Fig. 6. The proton single particle energies for $N = Z$ even-even mass nuclei in the case of the extended chiral sigma model without the pion mean field. The $1s_{1/2}$ orbit is pushed up, and the $N = 20$ magic number is shifted to $N = 18$. The spin orbit splitting between $0f_{7/2}$ and $0f_{5/2}$ is small, and the magic number at $N = 28$ is not visible.

as a function of r, which is defined as $U_{ls} = U_V - U_S$. The magnitude of this potential in the ECS model is about half of that in the TM1 case. The spin-orbit potential is then defined by eliminating the small component in the relativistic wave function and obtaining the spin-orbit operator explicitly as

$$V_{ls} = \frac{2}{r} \frac{\frac{d}{dr} U_{ls}}{(M + \varepsilon - U_{ls})^2} \vec{l} \cdot \vec{s}. \tag{4·13}$$

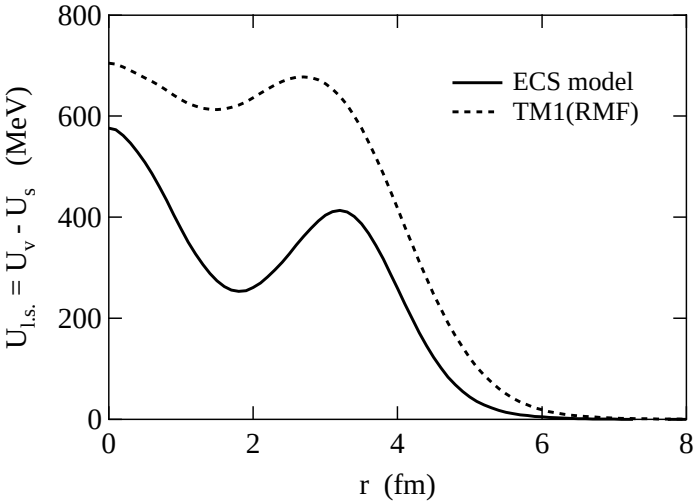

Fig. 7. The scalar-vector potential difference, U_{ls}, which is related to the spin-orbit potential, as a function of the radial coordinate, r. The potential difference for the case of the TM1 parameter set is represented by the dashed curve and that for the ECS model is represented by the solid curve.

The spin-orbit potential is proportional to the derivative of the scalar-vector potential difference, which emphasizes the contribution from the nuclear surface. Hence, to compare the magnitudes of the spin-orbit effects in the two cases, we calculate the volume integrals of V_{ls},

$$\int \frac{2}{r} \frac{\frac{d}{dr} U_{ls}}{(M + \varepsilon - U_{ls})^2} r^2 dr. \tag{4·14}$$

We use for ε the value corresponding to a binding energy of 8 MeV and obtain the ratio of these integrals in the two cases as 0.48, which is again about one half. Hence, the spin-orbit effect for the ECS model is about a half of that in the TM1 case. This was already evident from the single particle spectra shown in Fig. 6.

§5. Finite pion mean field for finite nuclei

We now include the pion mean field in the relativistic mean field calculation.[22),23)] The method of the numerical calculation is presented in the papers of Toki et al.[11)] and Sugimoto et al.[18)] The results for the binding energy per particle are shown in Fig. 4. In this calculation, we take $g_A = 1.15$ instead of the experimental axial coupling constant, $g_A = 1.25$, obtained using the Goldberger-Treimann relation. We take this smaller value in order to reproduce the binding energy for ^{56}Ni. It is very interesting that the magic number effect at $N = 28$ appears as the binding energy per particle increases at $N = 28$. This large effect of the finite pion mean field for jj-closed shell nuclei has been demonstrated in a previous work.[11)]

We give here an intuitive explanation to understand the energy curve of the magic structure presented in Fig. 4 in terms of the finite pion mean field using the

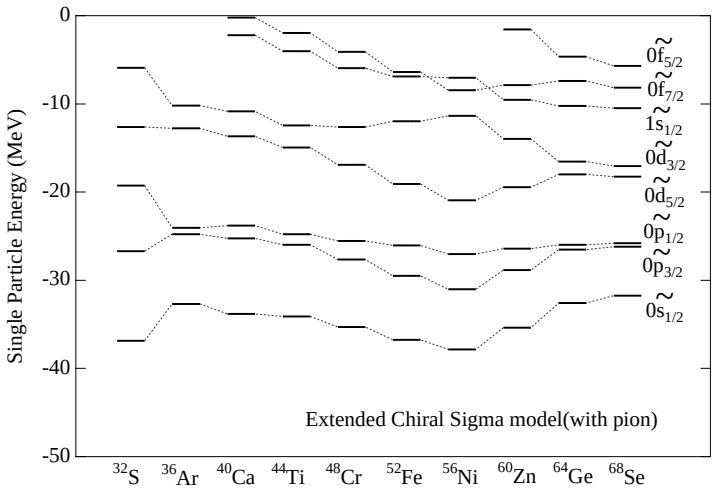

Fig. 8. The proton single particle energies for the $N = Z$ even-even mass nuclei in the case of the extended chiral sigma model with a pion mean field. The spin-orbit splitting is made large by the finite pion mean field, which is seen to be centered at the $N = Z = 28$ nucleus. We note that while the total angular momentum is a good quantum number, the angular momentum is not exact. For this reason we write the dominant angular momentum beside each single particle state.

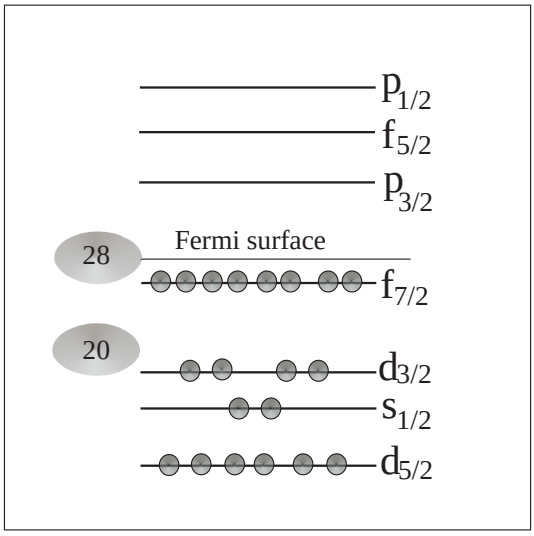

Fig. 9. A schematic picture of the single particle states and the occupied particles in the ^{56}Ni nucleus.

schematic picture in Fig. 9. To proceed, we have to first know the effect of the finite pion mean field in terms of the shell model. Analysis of the parity projection, carried out in a previous publication,[11] clearly shows that the pionic correlations due to the finite pion mean field can be expressed in terms of the coherent 0^- particle-hole excitations which are made by the coupling of the different parity states l and

$l' = l \pm 1$ with the same total spin j in the shell model language. In the analysis of the contribution to the pionic correlations from various single particle states, the highest spin state in each major shell has a special role. Only this highest spin state does not find a partner to form the 0^- state in the lower major shells. However, if this state is filled by nucleons, those nucleons are able to find 0^- partners in the higher major shells by creating particle-hole excitations. Hence, the position of the highest spin state in a major shell with respect to the Fermi surface is important in determining the strength of pionic correlations in nuclei.

In the case under consideration, the highest spin state is the $f_{7/2}$ state, as shown in Fig. 9. In the ^{40}Ca case, the occupied states cannot couple with the $f_{7/2}$ state to form 0^-, and the $f_{7/2}$ level plays no role in the pionic correlations. In the next case, i.e., that of ^{44}Ti, nucleons start to occupy the $f_{7/2}$ level, and these nucleons participate in the 0^- particle-hole excitations into $g_{7/2}$ levels. The number of particles involved in the pionic correlation increases as the nucleon number increases until ^{56}Ni, where the $f_{7/2}$ level is completely occupied. For nuclei above ^{56}Ni, the upper shells (i.e., those as high as $f_{5/2}$) become occupied, and those states do not participate in the 0^- particle-hole excitations from the $d_{5/2}$ level below caused by the pionic correlation due to Pauli blocking. For ^{56}Ni, the pionic correlation becomes maximal. This is the reason why ^{56}Ni realizes the largest pionic correlation energy, which leads to the appearance of the magic number at $N = 28$.

We now discuss the effect of the finite pion mean field on the single particle energies. We show in Fig. 8 the single particle spectra for various nuclei. We clearly see the large energy differences between the spin-orbit partners produced by the finite pion mean field as the energy differences become maximal for nuclei at $N = 28$. The pion mean field causes coupling of different parity states with the same total spin. The $0s_{1/2}$ and $0p_{1/2}$ states repel each other, and therefore the $0s_{1/2}$ state is pushed down and the $0p_{1/2}$ state is pushed up. The next set of partners consists of $0p_{3/2}$ and $0d_{3/2}$. The $0p_{3/2}$ state is pushed down, while the $0d_{3/2}$ state is pushed up. The next set of partners consists of $0d_{5/2}$ and $0f_{5/2}$. The $0d_{5/2}$ state is pushed down, while the $0f_{5/2}$ state is pushed up. This pion mean field effect continues to higher spin partners. This coupling of different parity states with the same total spin due to the finite pion mean field causes the splittings of the spin-orbit partners, as seen clearly for the $0p$ spin-orbit partners, the $0d$ spin-orbit partners and the $0f$ spin-orbit partners in ^{56}Ni. It is extremely interesting that the appearance of the energy splitting between the spin-orbit partners in the case of a finite pion mean field is caused completely by a different mechanism from that in the case of the spin-orbit interaction.

We now consider the contribution of each term in the Lagrangian for the cases with and without the pion mean field listed in Table I. The binding energy increases slightly when the pion mean field is made finite. The pion term contributes attractively, and the energy gain due to the pion term is obtained by making the kinetic energy and the sum of the sigma and omega potential terms increase. The structure of the wave functions changes significantly, while the total energy remains almost unchanged. This change of the structure causes the observables associated with the

Table I. The binding energy per particle (BE/A) and the contributions of the sum of the sigma and omega ($U_\sigma + U_\omega$), the kinetic (KE), pion (U_π), non-linear term (NL), sigma-omega coupling term (CP), and Coulomb (U_C) energies per nucleon in MeV for ^{56}Ni in the extended chiral sigma model.

	BE/A	$U_\sigma + U_\omega$	KE	U_π	NL	CP	U_C
with π field	8.6	−21.8	20.9	−2.9	8.1	−15.4	2.6
without π field	8.4	−22.6	18.8	0	8.0	−15.0	2.6

spin quantities to change greating. The effect of the structure change on various observables will be studied in the near future.

§6. Conclusion

We have studied infinite nuclear matter and finite nuclei with nucleon number $N = Z$ even-even mass in the range $N = 16 - 34$ using the chiral sigma model, which is good for hadron physics. The direct application of the chiral sigma model does not provide good saturation properties of infinite matter. We have therefore used the extended chiral sigma (ECS) model, in which the omega meson mass is dynamically generated by the sigma condensation as the nucleon mass. This ECS model is able to provide good saturation properties, although the predicted incompressibility is too large. Another characteristic property of the ECS model is that the scalar and vector potentials are about half as large as those in the case of the RMF(TM1) model for nuclear matter.

We then applied this ECS model to finite nuclei. The ECS model without a pion mean field gives the result that the magic number appears at $N = 18$, not at $N = 20$. This result comes from the large incompressibility found in the equation of state as $K = 650$ MeV. This property of the ECS model leads to a mean field central potential that is repulsive in the interior region and a $1s$-orbit that is significantly pushed up. Due to this, the magic number appears at $N = 18$ instead of $N = 20$. We note that this problem originates from the ECS model treated in the present framework, and the finite pion mean field in the mean field approximation does not remove this difficulty. There are several possibilities to solve this problem, such as treatments involving the effect of the Dirac sea, the parity projection, and the Fock term.

The ECS model without a pion mean field provides the result that the magic number does not appear at $N = 28$. This result comes from another characteristic property of the ECS model, which is the small scalar and vector potentials in nuclear matter. These scalar and vector potentials lead directly to the strength of the spin-orbit interaction in a finite system. Because the spin-orbit interaction given by the ECS model is about half as large as those obtained from the standard RMF calculation with the TM1 parameter set, the energy splittings between the spin-orbit partners are small, and therefore, there appears no magic effect at $N = 28$. Regarding this point, it is important to introduce the pion mean field by breaking the parity of the single particle states in the ECS model Lagrangian. Because the role of the pion mean field in the jj-closed shell nuclei is demonstrated in a previous

publication,[11] we have introduced the parity mixed intrinsic single particle states in order to treat the pion mean field in finite nuclei. We followed the formulation of Sugimoto et al.[18] in the RMF framework. We have found that the magic number effect appears at $N = 28$. We have studied the change of the single particle spectrum due to the finite pion mean field. It is extremely interesting that the spin-orbit partners are split significantly by the pion mean field effect. Specifically, the parity partners $s_{1/2}$ and $p_{1/2}$, $p_{3/2}$ and $d_{3/2}$, and $d_{5/2}$ and $f_{5/2}$ are pushed away from each other due to the pion mean field, and as a consequence, the spin-orbit partners are split by a large amount, like those of the ordinary spin-orbit splittings. This is related to the energy differences between the spin-orbit partners caused by the energy loss of the tensor (pionic) correlations due to the Pauli blocking.[24]

It is gratifying to observe that the extended chiral sigma model, which possesses chiral symmetry and its dynamical symmetry breaking, is able to produce the nuclear properties with only a small adjustment of the parameters in the Lagrangian. The energy splitting between the spin-orbit partners appears clearly in the ECS model with the pion mean field. The most important consequence obtained in this study is that this energy splitting is caused by the pion mean field, which is a completely different mechanism from that of the spin-orbit interaction introduced phenomenologically. This suggests the origin of the magic effect of jj-closed shell nuclei.

Acknowledgements

We acknowledge fruitful discussions with Prof. Y. Akaishi, Prof. H. Horiuchi and Prof. I. Tanihata on the role of the pion in nuclear physics. We are grateful to Dr. D. Jido for helpful discussions on the linear sigma model. We thank Prof. E. Oset for reading the manuscript and valuable discussions. This work is supported in part by a Grant-in-aid for Scientific Research [(B) 14340076] of the Ministry of Education, Culture, Sports, Science and Technology of Japan.

References

1) M. Gell-Mann and M. Levy, Nuovo Cim. **16** (1960), 705.
2) S. Weinberg, Phys. Rev. **166** (1968), 1568; ibid. **177** (1969), 2604.
3) Y. Nambu and G. Jona-Lasinio, Phys. Rev. **122** (1961), 345; ibid. **124** (1961), 246.
4) B. W. Lee, *Chiral Dynamics* (Gordon and Breach Science publishers).
5) H. Yukawa, Proc. Phys.-Math. Soc. Jpn. **17** (1935), 48.
6) J. D. Walecka, Ann. of Phys. **83** (1974), 491.
B. D. Serot and J. D. Walecka, in *Advances in Nuclear Physics*, ed. J. W. Negele and E. Vogt (Plenum Press, New York, 1986), vol. 16, p. 1.
7) J. Boguta, Phys. Lett. B **120** (1983), 34; ibid. **128** (1983), 19.
8) J. Kunz, D. Masak, U. Post and J. Boguta, Phys. Lett. B **169** (1986), 133.
9) V. N. Fomenko, S. Marcos and L. N. Savushkin, J. of Phys. **19** (1993), 545.
10) V. N. Fomenko, L. N. Savushkin, S. Marcos, R. Niembro and M. L. Quelle, J. of Phys. **21** (1995), 53.
11) H. Toki, S. Sugimoto and K. Ikeda, Prog. Theor. Phys. **108** (2002), 903.
12) Y. Sugahara and H. Toki, Nucl. Phys. A **579** (1994), 557.
13) A. Hosaka et al., to be published (2003).
14) K. Kawarabayashi and M. Suzuki, Phys. Rev. Lett. **16** (1996), 255.

15) A. Hosaka, Phys. Lett. B **244** (1990), 363.
16) O. Kaymakcalan, S. Rajeev and J. Schechter, Phys. Rev. D **30** (1984), 594.
17) Riazuddin and Fayyazuddin, Phys. Rev. **147** (1966), 1071.
18) S. Sugimoto, "Relativistic Mean Field Theory with Pion for Finite Nuclei", Docter thesis in Osaka University (2002).
19) R. Brockmann and R. Machleidt, Phys. Rev. C **42** (1990), 1965.
20) G. Ripka, Adv. Nucl. Phys. **1** (1968), 183.
21) H. Horiuchi and K. Ikeda, Int. Rev. Nucl. Phys. **4** (1985), 1.
22) H. Toki and W. Weise, Phys. Rev. Lett. **42** (1979), 1034.
23) E. Oset, H. Toki and W. Weise, Phys. Rep. **83** (1982), 281.
24) S. Takagi, W. Watari and M. Yasuno, Prog. Theor. Phys. **22** (1959), 549.
T. Terasawa, Prog. Theor. Phys. **23** (1960), 87.
A. Arima and T. Terasawa, Prog. Theor. Phys. **23** (1960), 115.